Forecasting short-term solar radiation for photovoltaic energy predictions

Forecasting short-term solar radiation for photovoltaic energy predictions

Alessandro Aliberti[1], Lorenzo Bottaccioli[1], Giansalvo Cirrincione[2],
Enrico Macii[1], Andrea Acquaviva[1] and Edoardo Patti[1]
[1]*Dept. of Control and Computer Engineering, Politecnico di Torino, Torino, Italy*
[2]*Universite de Picardie Jules Verne, Amiens, France*
{*alessandro.aliberti, lorenzo.bottaccioli, enrico.macii, andrea.acquaviva, edoardo.patti*}*@polito.it,*
{*giansalvo.cirrincione*}*@u-picardie.fr*

Keywords: Solar radiation forecast, Artificial neural networks, Photovoltaic system, Energy forecast, Renewable energy

Abstract: In the world, energy demand continues to grow incessantly. At the same time, there is a growing need to reduce CO_2 emissions, greenhouse effects and pollution in our cities. A viable solution consists in producing energy by exploiting renewable sources, such as solar energy. However, for the efficient use of this energy, accurate estimation methods are needed. Indeed, applications like Demand/Response require prediction tools to estimate the generation profiles of renewable energy sources.
This paper presents an innovative methodology for short-term (e.g. 15 minutes) forecasting of Global Horizontal Solar Irradiance (GHI). The proposed methodology is based on a Non-linear Autoregressive neural network. This neural network has been trained and validated with a dataset consisting of solar radiation samples collected for four years by a real weather station. Then GHI forecast, the output of the neural network, is given as input to our Photovoltaic simulator to predict energy production in short-term time periods. Finally, experimental results for both GHI forecast and Photovoltaic energy prediction are presented and discussed.

1 INTRODUCTION

The widespread development of Renewable Energy Sources (RES) in our cities, such as Photovoltaic (PV) systems, is changing the electrical energy production, consumption and distribution. Our society is facing the transition from centralized and hierarchical power distribution systems to distributed and cooperative ones, generally called Smart Grids. Smart Grid technologies are opening the electrical marketplace to new actors (e.g. prosumers and energy aggregators). Currently, power grid stability is achieved by classic generation plants using primary and secondary reserve at large-scale. Whilst, in a Smart Grid scenario, such a new actors can actively contribute to load balancing by fostering novel services for network management and stability. Demand/Response (Siano, 2014) is an example of application for Smart Grid management. It permits achieving a temporary virtual power plant (Vardakas et al., 2015) by changing the energy consumption pattern of consumers to match RES energy production or to fulfil grid operation requirements. This process is generally done every 15 minutes. To achieve these goals, prediction tools for both RES energy generation and consumption are needed.

In this work, we present a methodology for Photovoltaic energy prediction starting from forecasting short-term solar radiation. The forecast of solar radiation is obtained exploiting a Nonlinear Autoregressive neural network. We trained and validated this neural network with a dataset consisting of four years of Global Horizontal Solar Irradiance (GHI) samples collected by a real weather station. The neural network is a Multilayer Perceptron exploiting a high number of regressors to predict GHI in 15 minutes up to 2 hours range. Then, GHI forecast is given as input to our PV simulator that exploits GIS tools for simulating energy production. The rest of the paper is organized as follows. Section 2 reviews literature solution on solar radiation forecast. Section 3 introduces the followed methodology to define a neural network for short-term solar radiation forecasting. Section 4 details all the steps performed to initialize, train and validate our neural network. Section 5 discusses the results on solar radiation forecast. Section 6 describes the adopted Photovoltaic simulator. Section 6 presents also results and accuracy on PV

energy generation that exploits foretasted solar radiation given by the proposed neural network. Finally, Section 7 discusses concluding remarks.

2 RELATED WORK

Nowadays, solar energy represents a very attractive solution to produce green and clean energy. However, for an efficient conversion and utilization of solar power, solar radiation should be estimated and forecasted through accurate methods and tools. For example in Demand/Response applications (Siano, 2014), the amount of available energy must be known in advance to optimize the production of power plants (Aghaei and Alizadeh, 2013) and to match energy production with consumption. Hence, several studies were proposed in the literature to find mathematical and physical models to estimate and forecast the solar radiation, such as stochastic models based on time series (Kaplanis and Kaplani, 2016), (Voyant et al., 2014) and (Badescu, 2014). Moreover, classical linear time series models, like autoregressive moving average, have been widely used (Brockwell and Davis, 2016). However, it has been proven that these methodologies often are not sufficient in the analysis and prediction of solar radiation. This is due to the non-stationary and non-linearity of the solar radiation time series data (Madanchi et al., 2017), (Nazaripouya et al., 2016). Furthermore, stochastic models are based on the probability estimation. This leads to a difficult forecast of the solar radiation time series.

To overcome these limits, non-linear approaches, such as artificial neural networks (ANNs), were considered by many researchers as powerful methodologies to predict phenomenons, such as solar radiation (Voyant et al., 2017). Generally, ANNs do not require knowledge of internal system parameters. Furthermore, these models offer a compact solution for multiple variable problem (Qazi et al., 2015). However, also the use of an ANN to forecast a phenomenon introduces an error, the so-called *prediction error* (Yadav and Chandel, 2014). As a result, these models need optimizations to reduce this error.

With respect to literature solutions, the scientific novelty of the proposed methodology consists in using a neural network based on the Multilayer Perceptron to forecast solar radiation. Generally, most literature methodologies rely on the single past value to perform the forecast (Box et al., 2015). Whilst, the proposed solution allows to reduce significantly the *prediction error* by using a high number of regressors to perform predictions. In addition, we perform the forecast of solar radiation in short- and medium-term, i.e. from future 15 minutes up to next 2 hours.

3 METHODOLOGY

A time series identifies an ordered sequence of values of a variable at equally spaced time intervals (Hamilton, 1994). The usage of time series models brings two great benefits: i) understanding the underlying forces and structure that produced the observed data and ii) fitting a model and proceeding to forecast and monitor or even feedback and feed-forward control (Oancea and Ciucu, 2014).

3.1 The Multilayer Perceptron

Generally, one of the most effective methods for prediction based on time series consists in neural network (Montgomery et al., 2015), such as the Multilayer Perceptron (MLP), which is the artificial neural network most used in applications (Demuth et al., 2014). It is composed of units, called nodes or neurons, and organized in a layer of inputs, one or more hidden layers and an output layer. It is a feed-forward network with full connection between layers. The connections are characterized by adjustable parameters called weights. Hence, a weight refers to the strength of a connection between two nodes (Kubat, 2017). Each neuron computes a function of the sum of the weighted inputs. This function is called *activation function*.

In this work, we use an MLP-network architecture characterized by i) one hidden layer of neurons with hyperbolic tangent activation function f and ii) an output layer with a linear activation function F. The functional model is given by:

$$\begin{aligned} \hat{y}_i(w,W) &= F_i(\sum_{j=1}^{q} W_{ij} h_j + W_{i0}) = \\ &= F_i(\sum_{j=0}^{q} W_{ij} f_j(\sum_{l=1}^{m} w_{jl} u_l + w_{j0}) + W_{i0}) \end{aligned} \tag{1}$$

The weights are specified by the matrix $W = [W_{ij}]$ and by the matrix $w = [w_{jl}]$, where W_{ij} scales the connection between the hidden unit j and the output unit i and w_{jl} scales the connection between the hidden unit j and the input unit l. W_{i0} and w_{j0} are the corresponding biases. All this weights can be vectorized in a vector θ. The input units are represented by the vector $u(t)$ and the hidden neuron outputs are represented by the vector h. The outputs of the network, $\hat{y}_i$, are estimated by Eq. 1. The parameters are determined

during the *training process*, which requires a *training set* Z^N, composed of a set of inputs, $u(t)$, and corresponding desired outputs, $y(t)$, specified by:

$$Z^N = [u(t), y(t)],\ t = 1, ..., N \tag{2}$$

The training phase allows to determine a mapping from the set of training data to the set of possible weights:

$$Z^N \rightarrow \hat{\theta} \tag{3}$$

so that the network can produce prediction $\hat{y}(t)$, to be compared to the true output $y(t)$.

The *prediction error approach* is instead based on the introduction of a measure of closeness in terms of a mean square error criterion, as specified by:

$$V_N(\theta, Z^N) = \frac{1}{2N} \sum_{t=1}^{N} [y(t) - \hat{y}(t|\theta)]^T [y(t) - \hat{y}(t|\theta)] \tag{4}$$

The weights are then found as:

$$\hat{\theta} = arg_{\theta} min V_N(\theta, Z^N) \tag{5}$$

by some kind of iterative minimization scheme:

$$\theta^{i+1} = \theta^i + \mu^i + f^i \tag{6}$$

where θ^i specifies the current iteration, f^i the search direction and μ^i the step size.

3.2 System Identification

The following section details the adopted methodology to use an artificial neural network for short-term solar radiation predictions. Based on the process presented in (Norgaard et al., 2000), the procedure to identify a dynamical system consists of four steps: i) *Experiment*, ii) *Model Structure Selection*, iii) *Model Estimation* and iv) *Model Validation* (see Fig. 1).

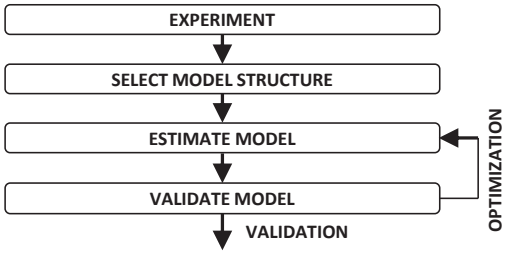

Figure 1: System identification procedure

Experiment This step corresponds to the problem analysis and the sampling and data collection. In neural network applications, once the scope has been identified, an adequate amount of data is needed. Generally, an higher number of data allows better forecasting performances (Srivastava et al., 2014). Then the available data must be divided into two different datasets: the training set and the validation set, respectively. These datasets are used in the training and validation phases of the neural network, which are the *Estimate Model* and the *Validate Model* steps in Fig. 1, respectively.

Model Structure Selection This step allows identifying the correct architecture model to use (Norgaard et al., 2000). Generally, this selection is more difficult in the nonlinear case than in the linear (Chandrashekar and Sahin, 2014). At this aim, the system regressor must be studied. In mathematical modeling, these regressors identify independent variables able to influence the dependent variables. In time series, then, these regressors represent previous samplings with respect to the predicted ones (Montgomery et al., 2015). Consequently, the best neural structure can be chosen.

Model Estimation In this step, once the network model and the number of regressors are identified, the network is first implemented and then trained. In time series scenario, training a neural network is needed to provide: i) the vector containing desired output data; ii) the number of regressors to define the prediction; iii) the vector containing the weights of both input-to-hidden and hidden-to-output layers and lastly iv) the data structure containing the parameters associated with the selected training algorithm. Finally, the training phase produces a *training error*, which represents the network performance index (Srivastava et al., 2014).

Model Validation This step validates the trained network. Generally, validating a network allows evaluating its capabilities (Miller et al., 1989). In time series predictions, the most common validation method consists of analysing the residuals (i.e. prediction errors) by cross-validating the test set. This method allows to perform a set of tests including also the autocorrelation function of the residuals and the cross-correlation function between controls and residuals. This analysis provides the *test error* (Srivastava et al., 2014), that is an index considered as a generalization of the error estimation. This index should not be too high compared to training error. If this happens, the network could over-fit the training set.

Network optimization and final validation Generally, if the network is over-fitting the training set, the

selected model structure contains too many weights. It is required to return in the *Estimate Model* step in order to change and redefine some structural parameters by optimizing the whole architecture. For this purpose, the superfluous weight must be pruned according to the Optimal Brain Surgeon (OBS) strategy, that represents one of the most important optimization strategies (Han et al., 2015). Consequently, once the new weights are given, the network architecture must be re-validated.

4 NAR NEURAL NETWORK FOR SHORT-TERM GHI FORECAST

In this work, we aim at forecasting the short-term Global Horizontal Solar Irradiance (GHI) for photovoltaic energy predictions. For this purpose, we used a dataset of about four years (from 2010 to 2013). It provides GHI values sampled every 15 minutes by the weather station in our University Campus. In detail, we considered all values in the time period from 8 a.m. to 6 p.m. Thus, we excluded evening and night time. Then, we split the dataset into training set (2010-2011) and validation set (2012-2013). This dataset appears to be statistically relevant. Nonetheless, we believe that if we could have used a larger accurate training set we could have achieved even more accurate prediction results. In order to deal with time series data, we adopted the Nonlinear Autoregressive neural network (NAR) belonging to the Nonlinear Autoregressive Exogenous Model (NARX) family (Siegelmann et al., 1997). Other choices, like NARMA (Norgaard et al., 2000) are possible. However, NARX is considered as the best tool in time series analysis (used as NAR) and does not suffer from stability problems. It is a nonlinear autoregressive model which has exogenous inputs. It is basically a choice of the inputs of a nonlinear model (an MLP neural network, as in (Norgaard et al., 2000)), which replaces the traditional linear model ARX (as in (Ljung, 1998)). It bases its predictions on i) past values of the series and ii) current and past values of the driving exogenous series, producing an error that represents the error of prediction. This error means that the knowledge of the past terms does not enable the future value of the time series to be predicted exactly. These network models are characterized by:

$$y_t = F(y_{t-1}, y_{t-2}, y_{t-3}, ..., u_t, u_{t-1}, u_{t-2}, u_{t-3}, ...) + \varepsilon_t \quad (7)$$

where y_t represents the variable of interest and u_t is the externally determined variable at time t respectively. In detail, information about u_t and previous values of u and y, helps predicting y_t, with a prediction error ε_t.

Once the model has been chosen, we analysed the number of past signals used as regressors for the prediction. We used *Lipschiz* method for determining the *lag-space* (Rajamani, 1998). This methodology allows identifying the orders of Input-Output Models for Nonlinear Dynamic Systems. However, as detailed in (He and Asada, 1993), this methodology is not always effective but it represents a good starting point to define the number of regressors. Fig. 2 details the result of the applied Lipschiz method, in which the number of past inputs is increased simultaneously from 1 to 20.

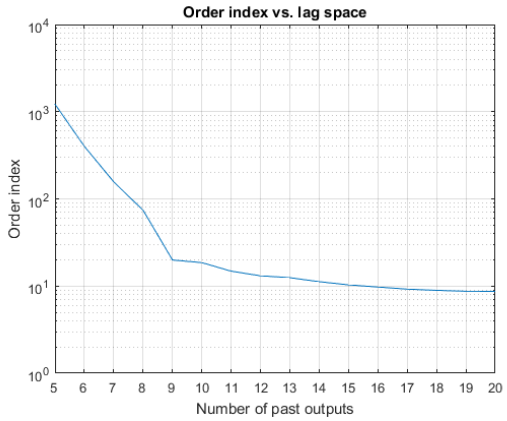

Figure 2: Evaluation of Order Index criterion for different lag-space

In this way, we deduced that the architecture can yield a good performance with only 9 regressors (i.e. 9 previous values for y and u, respectively, in Eq. 7). However, considering that the value of 10 is very close to the knee of the curve, 10 regressors have been chosen in order to have more conservative results, in the sense of the use of more information from the time series. Then, we chose an initial fully connected network architecture with one hidden layer of 30 hyperbolic tangent units. This large number of units is redundant, but justified by the pruning technique. The weights of the network are then initialized randomly before a training. This choice allows to initialize i) the weights, ii) their decay threshold and iii) the maximum number of iterations. However, these data structure parameters are overestimated during the first training. After this phase, we proceed training the neural network. Training is a minimization technique in order to compute the best weights for the network. Here we used the *Levenberg-Marquardt* algorithm, which interpolates between the Gauss-Newton algorithm and the method of gradient descent, using a *trust region* approach (Norgaard et al., 2000).

According to the purpose of this study, we chose to use the methodology illustrated in (Norgaard et al., 2002) for the network validation. This methodology allows the models systems validation of the outputs, performing a set of tests including autocorrelation function of the residuals and cross-correlation function between controls and residuals. This process produces the test error index as a result. The test error represents an estimation of the generalization error. This should not be too large compared to training error. If the test error (*NSSE*) is greater than the training error, it means that the predicted results are over-fitting the training set. In our case, the validation process yield this index equal to 3.27×10^3, which is a good value. Then, we proceeded to the optimization phase of the network. Our purpose was to remove excess weights and obtain a smaller training error than the one given during the first validation. In order to do so, we adopted the *Optimal Brain Surgeon* (OBS) strategy (Hansen et al., 1994), which prunes superfluous weights. OBS computes the Hessian matrix weights iteratively, which leads to a more exact approximation of the error function. The inverse Hessian is calculated by means of recursion. This method allows finding the smallest saliency S_i:

$$S_i = \frac{w_i^2}{2[H^{-1}]_{i,i}} \tag{8}$$

where $[H^{-1}]_{i,i}$ is the $(i,i)th$ element of the inverse Hessian matrix and w_i is the ith element of the vector θ containing network weights. The saliency identifies the quality of the connection between the various network units. This methodology allows to verify the state of the saliency iteratively. If the saliency S_i is much smaller than the mean-square error, then some synaptic weights are deleted and the remaining ones are updated. The computation stops when no more weights can be removed from the network without a large increase of the mean-square error. Once the new weights are given, we re-validated the network architecture.

Through the same methodology used in the first validation phase, we proceeded to the final network validation using the new weights. The resulting test error index NSSE was 3.11×10^3, that is lower than the previous one. Thus, the prediction error has been further lowered, giving more precise GHI forecast. Fig. 3 shows the final structure of the neural network after the optimization process.

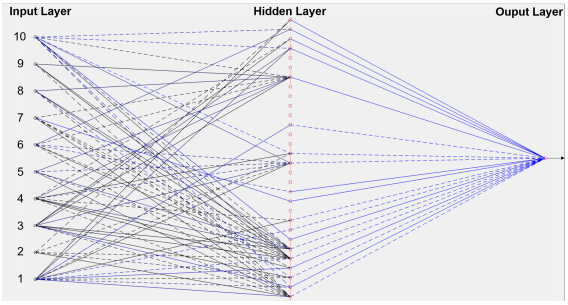

Figure 3: NAR optimized structure

5 RESULTS ON GHI FORECAST

The phases of the neural network characterization described in Section 4 allow defining an architecture that bases its prediction on 10 previous regressors. This represents a big advantage, as in literature these kinds of networks generally use just the single previous value to predict the next one. This implies a higher prediction error. In our case, by using a more large number of previous instances the prediction is good.

Our goal is to predict GHI in very short time windows (i.e. 15 minutes). We moved further predicting also GHI up to next two hours with 15 min. time interval. Using the dataset described in Section 4, we perform predictions by employing the methodology presented in (Norgaard et al., 2002). This methodology allows to determine the prediction value (that corresponds to the ahead k-step prediction of the system) and compare it to the measured output. The predictions are determined i) by feeding past predictions in the neural network where observations are not available and ii) by setting unavailable residuals to zero. Before starting the simulations, we set the prediction function to 10 regressors. In this section, we present the obtained results.

To evaluate the performance of our predictions, we used the indicators reported by Gueymard in (Gueymard, 2014). These indices of dispersion are: i) the *Root Mean Square Difference (RMSD)* that represents the standard deviation of differences between predicted and observed values; ii) the *Mean Absolute Difference (MAD)* that represents a measure of statistical dispersion obtained by the average absolute difference of two independent values drawn from a probability distribution; iii) the *Mean Bias Difference (MBD)* that measures the average squares of errors between predicted and measured values; iv) the *Coefficient of determination (r^2)* that represent the proportion between the variance and the predicted variable. *RMSD*, *MAD* and *MBD* are expressed in percentage rather than absolute units. Furthermore, we also con-

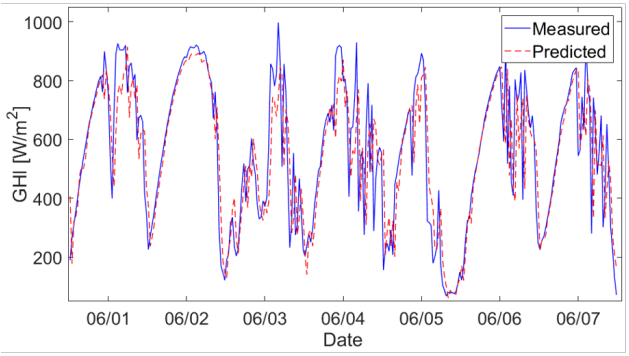

(a) $k = 1$

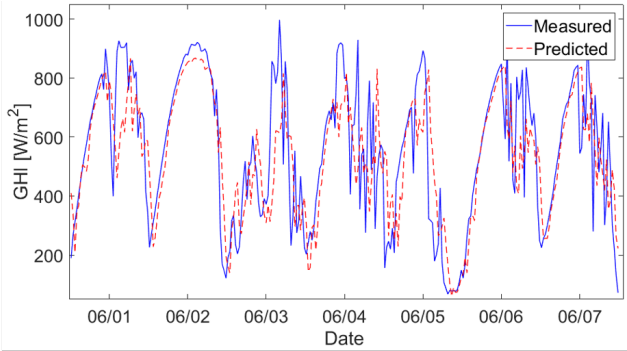

(b) $k = 2$

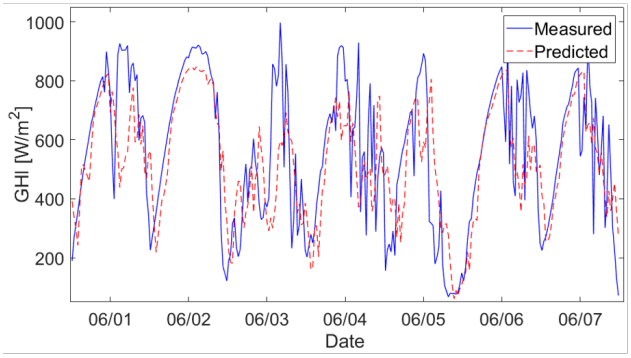

(c) $k = 3$

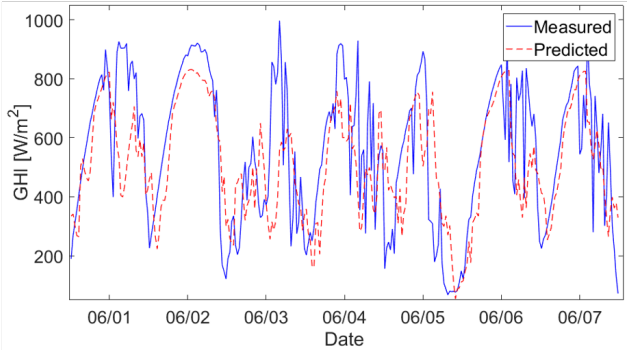

(d) $k = 4$

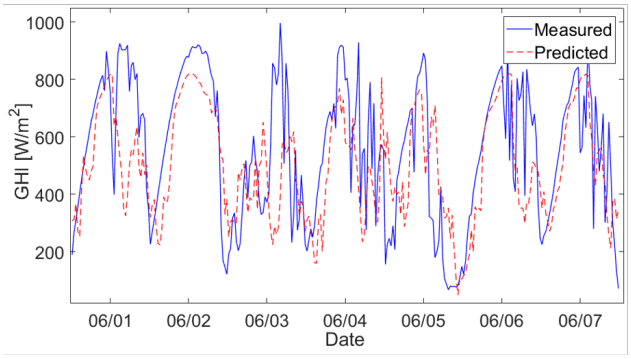

(e) $k = 5$

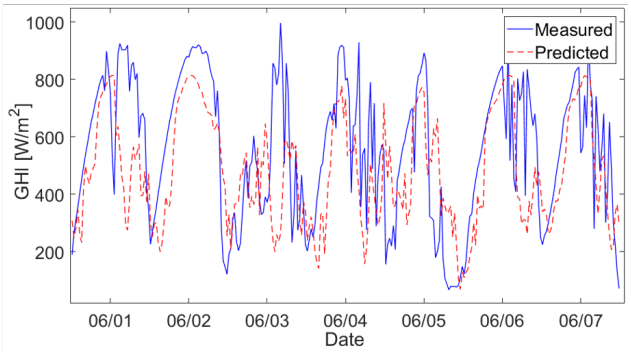

(f) $k = 6$

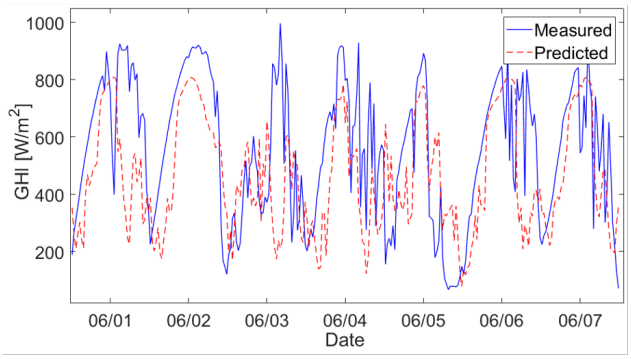

(g) $k = 7$

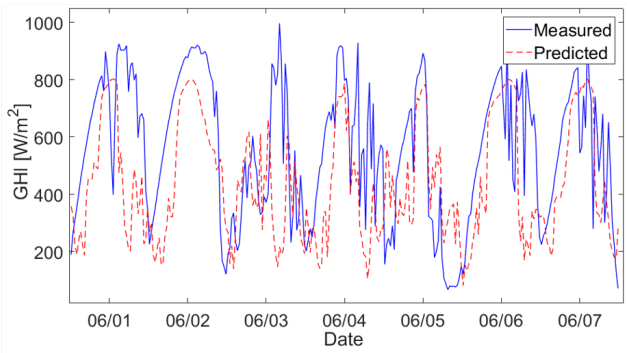

(g) $k = 8$

Figure 4: GHI prediction for $1 \leq k \leq 8$ (June 2013)

	Time [min]	MAD [%]	MDB [%]	r^2	RMSD [%]	LCE	WIA
k=1	15	13.56	0.26	0.91	25.37	0.81	0.98
k=2	30	19.82	0.70	0.84	32.92	0.72	0.96
k=3	45	24.28	1.08	0.80	37.61	0.66	0.94
k=4	60	28.02	1.27	0.75	41.55	0.60	0.93
k=5	75	31.30	1.52	0.71	45.10	0.56	0.91
k=6	105	34.43	1.42	0.66	48.48	0.51	0.90
k=7	115	37.88	0.97	0.61	52.15	0.46	0.88
k=8	120	41.32	0.14	0.55	55.97	0.41	0.86

Table 1: Performance Indicators for GHI prediction

sidered two indicators for the overall network performance: i) the *Willmotts Index of Agreement (WIA)* that represent the standardized measure of the degree of model prediction error (Willmott et al., 2012) and ii) the *Legatess Coefficient of Efficiency (LCE)* that is the ratio between the mean square error and the variance in the observed data (Legates and McCabe, 2013).

Fig. 4 shows the comparison among GHI results given by our neural network (dashed lines) and measured values sampled by the weather station (continues line) for different steps, from $k = 1$ (i.e next 15 min.) to $k = 8$ (i.e next 120 min.). These GHI predictions refer to the first week of June 2013. As shown in Fig. 4-(a), Fig. 4-(b) and Fig. 4-(c), the trends of our results for $1 \leq k \leq 3$ follow the real GHI behaviour with a good accuracy. Instead for $k > 3$, the prediction accuracy decreases (from Fig. 4-(d) to Fig. 4-(g)). This is also highlighted by Table 1 that reports the results of GHI predictions in terms of performance indicators considering the whole validation set (i.e. 2012-2013).

Performance indices clearly show that the architecture performance worsens by increasing the predictive steps. As a result, GHI prediction for high values of k has a greater error than real data. The analysis of indices highlights that the best GHI predictions are given at smaller intervals. For example, the *MAD* indicates that GHI prediction error grows as the prediction step k increases. Indeed, for prediction step $k = 1$ the error is about 13.6% while for $k = 8$ the error is around 41%. Also, *RMSD* has a similar trend. Furthermore, the *coefficient of determination* r^2 is much better than it is closer to 1. This index for prediction step $k = 1$ is equal to 0.91. Whilst, the error increases with an $r^2 = 0.55$ for $k = 8$.

This is also confirmed by *LCE* and *WIA* that highlight a decreasing of the overall performance on high prediction steps. Increasing the forecasting steps increase the errors and, consequently, the performances of prediction gets worst. Also for *LCE* and *WIA*, values closer to 1 represent the best case. For $k = 8$, *LCE* and *WIA* are equal to 0.41 and 0.86, respectively. However, the performance indexes for $1 \leq k \leq 3$ are acceptable to perform Photovoltaic energy estimations (see Section 6). In this scenario, the maximum error for GHI prediction is less than 25% for $k = 3$. The correctness of the choice of the number of regressors by the Lipschitz method seen previously is confirmed by the following additional analysis whose results are shown in Fig. 5. The technique proposed here has been repeated for different numbers of inputs and the corresponding NSSE has been recorded. It can be seen that too few regressors are not enough and seven or ten inputs give the best results. It confirms the choice in the proposed experiment.

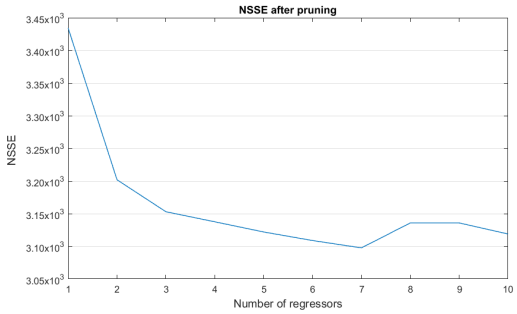

Figure 5: Evaluation of NSSE after pruning with regard to the number of regressors

6 PV ENERGY ESTIMATION

As discussed in Section 5, the results on GHI forecast are satisfactory especially on short-term time periods. This forecast of GHI allows estimating in advance the energy production of renewable, such as PV systems. In our case, we used GHI predictions as input to our PV energy simulator (Bottaccioli et al., 2017b). Estimating the PV production for the next short-term time windows enables the development of more accurate control policies for Smart Grid management, such as Demand/Response (Siano, 2014). Furthermore, this estimation allows to analyse the penetration level and the impact of renewable energy in existing districts and smart grids and. Also, to test and validate complex systems as presented in (Bottaccioli et al., 2017a).

6.1 PV simulator

This work exploits the software infrastructure presented in our previous work (Bottaccioli et al., 2017b) to estimate the energy generation profiles of PV systems in real-sky conditions. The inputs of this simulator are i) a *Digital Surface Model* (DSM) and ii) GHI trends. The DSM is a high-resolution raster image representing terrain elevation of buildings of interest.

It allows recognizing encumbrances on rooftops, such as chimneys and dormers, that prevent the deployment of PV panels. From the DSM, the PV simulator estimates the evolution of shadows in the rooftops over one year, with 15 minutes intervals. The result is the identification of the suitable area that is the available area on the rooftop where PV panels can be deployed.

The evolution of irradiance in real-sky conditions is given by combining GHI trends retrieved from personal or third-party weather stations (Weather Underground,) with the shadow model. In case of short-term prediction of PV energy production, the forecast of GHI trends is given by the proposed neural network (see Section 4). Then, the PV simulator decomposes GHI to estimate both Direct Normal Incident radiation (DNI) and Diffuse Horizontal Incident radiation (DHI) (Hofierka and Kaňuk, 2009). This decomposition is done by exploiting state-of-the-art decomposition models, such as (Engerer, 2015) and (Ruiz-Arias et al., 2010), and considering the attenuation caused by air pollution applying the *Linke turbidity coefficient* (Linke, 1922). Finally, the PV energy production is given by applying the methodology presented in (Brihmat and Mekhtoub, 2014).

6.2 Results on PV generation forecast

In this section, we present the results of PV generation forecast in short-term time periods. In this scenario, the PV simulator exploits GHI trends given by the proposed neural network (see Section 4) with different time steps: i) $k = 1$ (i.e next 15 min.), ii) $k = 2$ (i.e next 30 min.) and iii) $k = 3$ (i.e next 45 min.). To evaluate the errors of this approach, we repeated the PV simulations with real GHI trends sampled by the weather station in our campus. Fig. 6reports the plots of the instant power for three generic days in June 2013: i) sunny, ii) cloudy and iii) rainy. Generally, the trends of our results with GHI forecast (dashed line) follow with a good accuracy the behaviour of measured GHI (continues line). As expected, simulations with $k = 1$ performs better than simulations with $k = 2$ and $k = 3$. As shown in the three plots in Fig. 6, PV energy simulations are more affected by errors during rainy days especially during the early hours in the morning. This is because the algorithm expects higher GHI values. However, the algorithm is also able to recognize the wrong GHI estimation and correct the error after few time-steps.

Table 2 reports the performance indicators for simulations with $1 \leq k \leq 3$ with respect to simulations with sampled GHI trends. The performance indicators show that increasing the predictive steps (k)

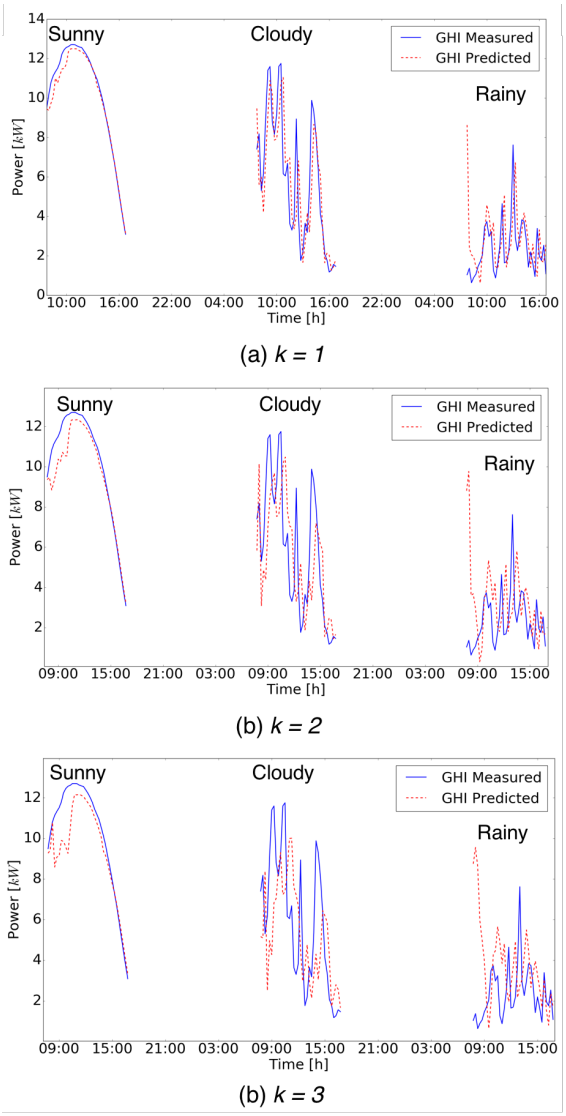

Figure 6: Simulations of PV energy production with $k = 1$ and $k = 2$ (June 2013)

	Time [min]	MAD [%]	MDB [%]	r^2	RMSD [%]	LCE	WIA
k=1	15	11.33	-0.70	0.91	21.34	0.82	0.98
k=2	30	16.87	-0.81	0.84	28.81	0.73	0.96
k=3	45	20.97	-0.86	0.77	34.28	0.67	0.94

Table 2: Performance Indicator for PV simulation

the accuracy on the results decreases. *MAD* increases from 11.33% for $k = 1$ to 20.97% for $k = 3$. Also *RMSD* has a similar trend. r^2 for prediction step $k = 1$ is equal to 0.91. Whilst, the error increases with an $r^2 = 0.77$ for $k = 3$. Finally, LCE varies from 0.82 to 0.67 and WIA decreases from 0.98 to 0.94.

These results confirm that PV simulations with GHI trends for $1 \leq k \leq 3$ given by the proposed neural

network are acceptable to estimate the energy production in the short-term time periods.

7 CONCLUSIONS

In this paper, we presented a methodology to forecast the short-term solar radiation, suitable for photovoltaic energy predictions. We discussed the results of the neural network forecast, introducing the NAR architecture able to base its prediction on a high number of regressors. Furthermore, we compared our results with real GHI values sampled by a real weather station in our University campus. The analysis of performance indicators highlighted an overall good performance in predicting the solar radiation, especially for the next 15, 30 and 45 minutes. As discussed, this short-term forecast of solar radiation allows estimating in advance the energy production of PV systems with a good accuracy. This enables the design of more accurate control policies for smart grids management, such as Demand/Response.

ACKNOWLEDGEMENTS

This work was partially supported by the EU project FLEXMETER and by the Italian project "Edifici a Zero Consumo Energetico in Distretti Urbani Intelligenti".

REFERENCES

Aghaei, J. and Alizadeh, M.-I. (2013). Demand response in smart electricity grids equipped with renewable energy sources: A review. *Renewable and Sustainable Energy Reviews*, 18:64–72.

Badescu, V. (2014). *Modeling solar radiation at the earth's surface*. Springer.

Bottaccioli, L., Estebsari, A., Patti, E., Pons, E., and Acquaviva, A. (2017a). A novel integrated real-time simulation platform for assessing photovoltaic penetration impacts in smart grids. *Energy Procedia*, 111:780–789.

Bottaccioli, L., Patti, E., Macii, E., and Acquaviva, A. (2017b). Gis-based software infrastructure to model pv generation in fine-grained spatio-temporal domain. *IEEE Systems Journal*.

Box, G. E., Jenkins, G. M., Reinsel, G. C., and Ljung, G. M. (2015). *Time series analysis: forecasting and control*. John Wiley & Sons.

Brihmat, F. and Mekhtoub, S. (2014). Pv cell temperature/pv power output relationships homer methodology calculation. In *International Journal of Scientific Research & Engineering Technology*, volume 1. International Publisher &C. O.

Brockwell, P. J. and Davis, R. A. (2016). *Introduction to time series and forecasting*. springer.

Chandrashekar, G. and Sahin, F. (2014). A survey on feature selection methods. *Computers & Electrical Engineering*, 40(1):16–28.

Demuth, H. B., Beale, M. H., De Jess, O., and Hagan, M. T. (2014). *Neural network design*. Martin Hagan.

Engerer, N. (2015). Minute resolution estimates of the diffuse fraction of global irradiance for southeastern australia. *Solar Energy*, 116:215–237.

Gueymard, C. A. (2014). A review of validation methodologies and statistical performance indicators for modeled solar radiation data: Towards a better bankability of solar projects. *Renewable and Sustainable Energy Reviews*, 39:1024–1034.

Hamilton, J. D. (1994). *Time series analysis*, volume 2. Princeton university press Princeton.

Han, S., Pool, J., Tran, J., and Dally, W. (2015). Learning both weights and connections for efficient neural network. In *Advances in Neural Information Processing Systems*, pages 1135–1143.

Hansen, L. K. et al. (1994). Controlled growth of cascade correlation nets. In *ICANN94*, pages 797–800. Springer.

He, X. and Asada, H. (1993). A new method for identifying orders of input-output models for nonlinear dynamic systems. In *American Control Conference, 1993*, pages 2520–2523. IEEE.

Hofierka, J. and Kaňuk, J. (2009). Assessment of photovoltaic potential in urban areas using open-source solar radiation tools. *Renewable Energy*, 34(10):2206–2214.

Kaplanis, S. and Kaplani, E. (2016). Stochastic prediction of hourly global solar radiation profiles.

Kubat, M. (2017). Artificial neural networks. In *An Introduction to Machine Learning*, pages 91–111. Springer.

Legates, D. R. and McCabe, G. J. (2013). A refined index of model performance: a rejoinder. *International Journal of Climatology*, 33(4):1053–1056.

Linke, F. (1922). Transmissions-koeffizient und trübungsfaktor. *Beitr. Phys. Fr. Atmos*, 10:91–103.

Ljung, L. (1998). System identification. In *Signal analysis and prediction*, pages 163–173. Springer.

Madanchi, A., Absalan, M., Lohmann, G., Anvari, M., and Tabar, M. R. R. (2017). Strong short-term nonlinearity of solar irradiance fluctuations. *Solar Energy*, 144:1–9.

Miller, G. F., Todd, P. M., and Hegde, S. U. (1989). Designing neural networks using genetic algorithms. In *ICGA*, volume 89, pages 379–384.

Montgomery, D. C., Jennings, C. L., and Kulahci, M. (2015). *Introduction to time series analysis and forecasting*. John Wiley & Sons.

Nazaripouya, H., Wang, B., Wang, Y., Chu, P., Pota, H., and Gadh, R. (2016). Univariate time series prediction of solar power using a hybrid wavelet-arma-narx

prediction method. In *Transmission and Distribution Conference and Exposition (T&D), 2016 IEEE/PES*, pages 1–5. IEEE.

Norgaard, M., Ravn, O., and Poulsen, N. K. l. (2002). Nnsysid-toolbox for system identification with neural networks. *Mathematical and computer modelling of dynamical systems*, 8(1):1–20.

Norgaard, P. M., Ravn, O., Poulsen, N. K., and Hansen, L. K. (2000). Neural networks for modelling and control of dynamic systems-a practitioner's handbook.

Oancea, B. and Ciucu, Ş. C. (2014). Time series forecasting using neural networks. *arXiv preprint arXiv:1401.1333*.

Qazi, A., Fayaz, H., Wadi, A., Raj, R. G., Rahim, N., and Khan, W. A. (2015). The artificial neural network for solar radiation prediction and designing solar systems: a systematic literature review. *Journal of Cleaner Production*, 104:1–12.

Rajamani, R. (1998). Observers for lipschitz nonlinear systems. *IEEE transactions on Automatic Control*, 43(3):397–401.

Ruiz-Arias, J., Alsamamra, H., Tovar-Pescador, J., and Pozo-Vzquez, D. (2010). Proposal of a regressive model for the hourly diffuse solar radiation under all sky conditions. *Energy Conversion and Management*, 51(5):881 – 893.

Siano, P. (2014). Demand response and smart gridsa survey. *Renewable and Sustainable Energy Reviews*, 30:461–478.

Siegelmann, H. T., Horne, B. G., and Giles, C. L. (1997). Computational capabilities of recurrent narx neural networks. *IEEE Transactions on Systems, Man, and Cybernetics, Part B (Cybernetics)*, 27(2):208–215.

Srivastava, N., Hinton, G. E., Krizhevsky, A., Sutskever, I., and Salakhutdinov, R. (2014). Dropout: a simple way to prevent neural networks from overfitting. *Journal of machine learning research*, 15(1):1929–1958.

Vardakas, J. S., Zorba, N., and Verikoukis, C. V. (2015). A survey on demand response programs in smart grids: Pricing methods and optimization algorithms. *IEEE Communications Surveys & Tutorials*, 17(1):152–178.

Voyant, C., Darras, C., Muselli, M., Paoli, C., Nivet, M.-L., and Poggi, P. (2014). Bayesian rules and stochastic models for high accuracy prediction of solar radiation. *Applied Energy*, 114:218–226.

Voyant, C., Notton, G., Kalogirou, S., Nivet, M.-L., Paoli, C., Motte, F., and Fouilloy, A. (2017). Machine learning methods for solar radiation forecasting: A review. *Renewable Energy*, 105:569–582.

Weather Underground. http://www.wunderground.com.

Willmott, C. J., Robeson, S. M., and Matsuura, K. (2012). A refined index of model performance. *International Journal of Climatology*, 32(13):2088–2094.

Yadav, A. K. and Chandel, S. (2014). Solar radiation prediction using artificial neural network techniques: A review. *Renewable and Sustainable Energy Reviews*, 33:772–781.